



1 **Model-based analysis of erosion-induced microplastic delivery from arable land to the**
2 **stream network of a mesoscale catchment**

3 Raphael Rehm^a, Peter Fiener^a

4 ^a University of Augsburg, Institute of Geography, *Alter Postweg 118, 86159 Augsburg,*
5 *Germany*

6 *Correspondance to:* Peter Fiener (peter.fiener@geo.uni-ausburg.de)

7



8 **Abstract**

9 Soils are generally accepted as sinks for microplastic (MP), but at the same time might be a MP source
10 for inland waters. However, little is known regarding the potential MP delivery from soils to aquatic
11 systems via surface runoff and erosion. This study provides for the first time an estimate of the extent of
12 soil erosion-induced MP delivery from an arable-dominated mesoscale catchment (390 km²) to its river
13 network within a typical arable region of Southern Germany. To do this, a soil erosion model was used
14 and combined with potential particular MP load on arable land from different sources (sewage sludge,
15 compost, atmospheric deposition and tyre wear) since 1950. The modelling resulted in an annual mean
16 MP flux into the stream network of 6.33°kg° in 2020, which was dominated by tyre wear (80%). Overall,
17 0.11–0.17% of the MP applied to arable soils between 1950 and 2020 was transported into the stream
18 network. In terms of mass, this small proportion was in the same range as the MP inputs from wastewater
19 treatment plants within the test catchment. More MP (0.5–1% of input between 1950 and 2020) was
20 deposited in the grassland areas along the stream network, and this could be an additional source of MP
21 during flood events. Most (5% of the MP applied between 1950 and 2020) of the MP translocated by
22 tillage and water erosion was buried under the plough layer. Thus, the main part of the MP added to
23 arable land remained in the topsoil and is available for long-term soil erosion. This can be illustrated
24 based on a ‘stop MP input in 2020’ scenario, indicating that MP delivery to the stream network until
25 2100 would only be reduced by 14%. Overall, arable land at risk of soil erosion represents a long-term
26 MP sink, but also a long-term MP source for inland waters.

27



28 **1. Introduction**

29 The global microplastic (MP) contamination of different environmental compartments is currently the
30 focus of different research fields (Nasseri and Azizi, 2022; Tian et al., 2022; Zhang et al., 2022). Among
31 these, MP in soils have increasingly received scientific attention (Chia et al., 2021; Sajjad et al., 2022;
32 Zhou et al., 2020). Many MP sources have been identified for soil systems. Next to tyre wear (TW),
33 stated as the main source (Knight et al., 2020; Sommer et al., 2018), littering (Scheurer and Bigalke,
34 2018) and atmospheric deposition (Brahney et al., 2020) also serve as MP input pathways. Arable soils
35 in particular experience increased MP inputs as a result of agricultural management (Brandes, 2020).
36 Mulch films (Ng et al., 2020), the use of compost and sewage sludge as organic fertilizers (Braun et al.,
37 2021; Liu et al., 2014; Zhang et al., 2020), irrigation with contaminated (waste) water (Pérez-Reverón et
38 al., 2022), as well as MP associated with coated fertilizer and seeds (Accinelli et al., 2021; Lian et al.,
39 2021), have proven to be the main input paths. MP enters the soil system mostly via the surface and is
40 mixed into the soil column via bioturbation (Heinze et al., 2022; Li et al., 2021) and, in the case of small
41 particles, via infiltration (Li et al., 2021). In arable land, it is actively mixed into the plough layer via
42 tillage operations (Weber et al., 2022; Zhao et al., 2022; Zubris and Richards, 2005). Depending on the
43 tillage technique, the MP is worked into the soil at different depths and is more or less homogenized after
44 multiple processing (Fiener et al., 2018; Weber et al., 2022). Moreover, tillage potentially leads to
45 mechanical fragmentation of macroplastic but also reduces photochemical decomposition at the soil
46 surface and reduces MP transport via water and wind (Colin et al., 1981; Corcoran, 2022; Feuilleley et
47 al., 2005).

48 Despite the known pathways into the soil, knowledge of the fate of MP particles once they enter the
49 soil system is limited (Guo et al., 2020; Hurley and Nizzetto, 2018; Tian et al., 2022). However, the
50 question arises as to whether the terrestrial MP sink releases relevant amounts of MP for water bodies
51 via water erosion. If so, the soils, as an MP sink, could represent an important MP source for water



52 bodies. Besides very slow, not very well determined processes of plastic fragmentation (Corcoran, 2022),
53 there is also only a small number of studies analysing vertical MP transport due to bioturbation (Heinze
54 et al., 2022; Li et al., 2021) and leaching (Chia et al., 2021; Viaroli et al., 2022) within the soil column,
55 or lateral losses to other ecosystems via erosion processes (Borthakur et al., 2022; Bullard et al., 2021;
56 Rehm et al., 2021).

57 The potential lateral transport via (water) erosion processes might be analysed using existing
58 modelling techniques. Such approaches face two major challenges: modelling approaches are required
59 which allow the cumulative loss of MP to adjacent ecosystems to be determined while taking spatial
60 differences in MP contamination and site-specific erosion into account. Moreover, the long-term change
61 in MP concentrations in the plough layer should be considered, following mixing with subsoil at
62 erosional sites or burial of MP below the plough layer at depositional sites.

63 In general, there are different water erosion modelling approaches available, ranging from physically-
64 oriented models (MCST, Fiener et al., 2008; e.g. EROSION3D, Schmidt et al., 1999), which might be
65 suitable for dealing with the specific particle size and density of MP during transport in the case of
66 individual erosion events, to conceptual approaches (e.g. WaTEM/SEDEM, (Van Oost et al., 2000; Van
67 Rompaey et al., 2001), which are able to consider long-term cumulative MP soil contamination and the
68 associated long-term soil and MP erosion, transport and deposition. In general, models of the first type
69 are very parameter and input data intensive and are mostly applied in small catchments, while the second
70 type of model needs less detailed data and is often used for mesoscale catchments (Nunes et al., 2018).
71 Following the requirements outlined above, conceptual, long-term approaches that account for spatial
72 variability in MP soil contamination and erosion processes seemed to be more appropriate than process-
73 oriented models to simulate the magnitude of erosion-induced MP delivery to the stream network of
74 mesoscale catchments. As MP loss below the plough layer might be also important in reducing topsoil
75 MP contamination, such a model approach should not only simulate water erosion, but also tillage



76 erosion processes leading to a reduction of the MP concentration at erosional sites and MP burial below
77 the plough layer at depositional sites. One of the few models simulating long-term water and tillage
78 erosion in a spatial context that updates the soil properties within the soil profile is the SPEROS-C model
79 (Fiener et al., 2015; Van Oost et al., 2005b). The water and tillage erosion components of the model,
80 originating from the WaTEM/SEDEM model (Van Oost et al., 2000; Van Rompaey et al., 2001), were
81 tested in several micro- and mesoscale catchments (Krasa et al., 2005; Verstraeten and Prosser, 2008).

82 The general objective of this study is to investigate MP transport from arable land to the stream
83 network in an example mesoscale (390 km²) arable catchment in Southern Germany. Therefore, the
84 SPEROS-C carbon transport model was adjusted to study the importance of water and tillage erosion
85 processes for particular MP transport. Specifically, this study focuses on the following areas: (i)
86 quantifying the importance of the water erosion pathway for MP input to the stream network in an
87 example mesoscale catchment, while taking into account the large uncertainties, particularly in estimates
88 of MP input to soil; (ii) determining the importance of different erosion processes in changing the MP
89 concentration in the plough layer and burying MP below the plough layer, and (iii) using scenarios to
90 determine future pathways of diffuse MP delivery into the stream network.

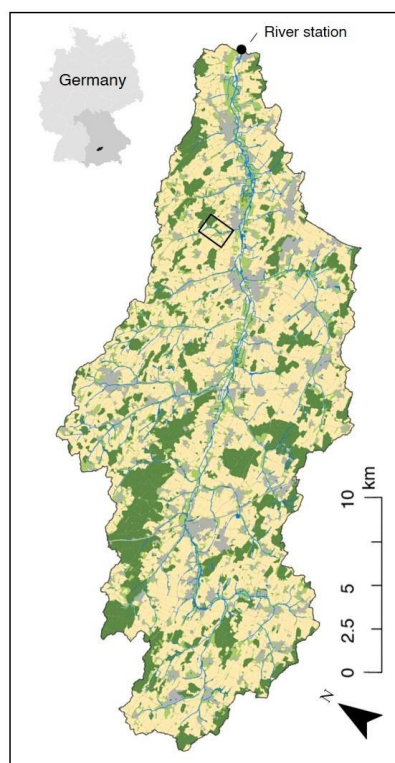
91 **2. Methods**

92 *2.1. Test catchment*

93 The catchment was chosen for two main reasons: (i) it represents an intensively used arable landscape
94 in Southern Germany with hilly terrain and highly productive, loess-burden soils, and (ii) the Bavarian
95 States Office for Environment has monitored discharge and sediment delivery at the outlet since 1968,
96 which allows the erosion component of the model to be tested. The mesoscale Glonn catchment
97 (48°22'N, 11°24'E) covers 390 km² and its altitude ranges from 578 m in its south-west to 447 m a.s.l.
98 at its outlet in the north-east (Fig. 1). Mean annual temperature and mean precipitation of the region are



99 7.5°C and 876 mm respectively, with the most intense rainfall events associated with convective rainfall
100 in summer. The hilly landscape ($4.7 \pm 3.7^\circ$ main slope) is characterized by loamy Cambisols (WRB, 2015)
101 on the elevated terrain and loamy Gleysols (WRB, 2015) in the valleys. Land cover in this area is
102 dominated by arable land (54%), followed by forest (21%), grassland (14%) and settlements (11%) (Fig.
103 1). The main crops are arranged in a corn-grain rotation. Due to the topography and the soils, erosion
104 rates reach values of about $10 \text{ t ha}^{-1} \text{ a}^{-1}$ (Auerswald et al., 2009).



105

106 **Figure 1: The Glonn catchment (390 km²) representing a typical intensively used arable landscape**
107 **in Southern Germany. The black rectangle within the catchment marks the section of the detailed**
108 **maps in Fig. 7.**

109



110 *2.2. Model*

111 The erosion and MP transport is modelled based on a modified version of the spatially distributed
112 water and tillage erosion and carbon (C) turnover model SPEROS-C (Fiener et al., 2015; Van Oost et
113 al., 2005a). The model was originally developed to analyse the long-term effect of soil erosion on
114 landscape-scale carbon balance (e.g. Nadeu et al., 2015), whereas the erosion components are based on
115 the erosion and sediment transport model WaTEM/SEDEM, which was extensively tested and validated
116 in different regions of the world (Krasa et al., 2005; Van Oost et al., 2000; Van Rompaey et al., 2001;
117 Verstraeten and Prosser, 2008). The most important model components for this study are: (i) the water
118 erosion and sediment transport component, (ii) the tillage erosion component, and (iii) the lateral
119 redistribution and the vertical mixing of MP in the soil profile following erosion and deposition
120 processes. As the C turnover component of SPEROS-C was not used in this study but the MP component
121 was introduced, the model will subsequently be referred to as SPEROS-MP.

122 *Water erosion component:* The water erosion component of SPEROS-MP consists of two main parts.
123 First, the erosion potential of each raster cell (5 m x 5 m) is estimated based on the German version of
124 the Universal Soil Loss Equation ABAG (Schwertmann et al., 1987). The major advantage of this well-
125 tested approach is that the input data to calculate the different USLE (ABAG) factors are available from
126 the Bavarian State Office of Agriculture (Bayerische Landesanstalt für Landwirtschaft; LfL) and are
127 regularly updated by the State Office administration. Sediment transport per raster cell, and hence
128 deposition if transport capacity is smaller than sediment influx, is calculated using Eq. 1:

129
$$T_c = k_{tc} \cdot R \cdot C \cdot K \cdot LS_{2D} \cdot P \quad (\text{Eq. 1})$$

130 Where T_c is the transport capacity ($\text{kg m}^{-1} \text{a}^{-1}$), k_{tc} is the transport coefficient; R ($\text{N h}^{-1} \text{a}^{-1}$), C (-), K (kg
131 $\text{h m}^{-2} \text{N}^{-1}$) and P (-) are the rainfall erosivity, soil cover, soil erodibility, and management factors of the



132 USLE calculated for Bavaria following the approach of Fiener et al. (2020). LS_{2D} is a grid cell-specific
133 topographic combined slope gradient and lengths factor calculated following Desmet and Govers (1996,
134 using the digital elevation model (DEM) with a resolution of 5 m x 5 m.

135 *Tillage erosion component:* Tillage erosion is calculated based on a diffusion-type equation adopted
136 from (Govers et al., 1994)), which generally assumes that tillage erosion is proportional to slope gradient.
137 Consequently, tillage erosion or deposition is most prominent if slope gradient changes, with most soil
138 loss modelled at convexities and most soil accumulation at concavities. Tillage erosion has no direct
139 effect on sediment or MP delivery into the stream network, but over time it modifies the MP
140 concentration in the plough layer of different raster cells, leading to a decrease in MP delivery, because
141 at erosional sites subsoil with little potential MP is mixed into the plough layer, while MP at depositional
142 sites is buried below the plough layer.

143 *MP redistribution and vertical mixing:* It is generally assumed that MP is entering the soil via its
144 surface and is immediately mixed into the plough layer (upper 0.2 m). The MP input to arable land is
145 estimated at field level (see input estimate below). For MP erosion the concentration in the plough layer
146 of each 5 m x 5 m raster cell was multiplied with the bulk soil erosion of this raster cell to calculate the
147 MP outflux to neighbouring cells. The MP concentration of the transported sediment is analogously used
148 to calculate potential MP deposition. After each year of modelling water and tillage erosion, the soil
149 profile is updated assuming a tillage operation to a constant depth of 0.2 m. Consequently, MP-free
150 subsoil is mixed into the plough layer at erosional sites, decreasing the topsoil MP concentration, while
151 at depositional sites the deposited MP is mixed with the underlying old plough layer, creating a new
152 topsoil MP concentration and some MP in the layer no longer reached by the plough. Over the years this
153 creates a steadily increasing variability in MP concentration within fields and transports MP into soils of
154 other land uses (e.g. grassland and forest sites) assumed not to get other MP inputs.



155 *2.3. Data*

156 *2.3.1. Soil erosion model inputs and parameters*

157 For the study area, the LfL provided a digital elevation model (DEM, raster 5 m x 5 m), land-use data
158 (field based) and a soil map (1:25,000) as well as most USLE factors (Tab. 1). A transport capacity
159 coefficient k_{tc} of 150 m was used as the optimum value for cropland for a 5 m x 5 m grid resolution
160 (Dlugoß et al., 2012). For the sake of simplicity and because long-term data on soil management was
161 missing, only the rainfall erosivity (R factor of the USLE) was calculated on a yearly basis, following
162 the approach of Schwertmann et al. (1987, using the mean annual precipitation N (mm/a). N was
163 available in a 1 km x 1 km grid resolution from the German Weather Service (DWD, 2020). We assumed
164 a corn-grain crop rotation (with a mixture of small grain crops and a proportion of row crops of 25%)
165 typically found in the region and used the USLE calculator developed by Brandhuber et al. (2018,
166 resulting in a C factor of 0.15, which is constantly used for all arable land in the catchment (Tab. 1). In
167 the case of forest and grassland, a low C factor of 0.004 and for settlements a C factor of 0.001 was
168 applied (Brandhuber et al., 2018). A K factor map was provided by the LfL (derived from the soil
169 properties given by the soil overview map of Bavaria at a scale of 1:25,000) based on the calculation in
170 Schwertmann et al. (1987). The LS_{2D} factor was derived from the 5 m x 5 m DEM, following the approach
171 of Desmet and Govers (1996. Assuming some soil conservation methods to be in place, e.g. partial
172 contour ploughing, the P factor was set to 0.85 (Fiener et al., 2020). The tillage transport coefficient k_{til}
173 depends on the tillage implement, tillage speed, tillage depths, bulk density, texture and soil moisture at
174 time of tillage (Van Oost et al., 2006). For the tillage erosion modelled, a constant k_{til} value of 350 kg m⁻¹
175 a⁻¹ for all fields was assumed (Tab. 1), which is a conservative estimate of a mixture of mouldboard
176 and chisel ploughing (Van Oost et al., 2006).



177 **Table 1: USLE factors used in SPEROS-MP.**

Factors of the USLE	Value	Unit	Comment	Reference
k_{tc}	150	m		<i>Dlugoß et al., 2012</i>
R	0.048-0.089	$N\ h^{-1}\ a^{-1}$	Varies annually, controls the variability of the model	<i>DWD (2020)</i>
<i>C</i>				
<i>Arable land</i>	0.15	-	Does not vary spatially within different land uses	<i>Brandhuber et al., 2018</i>
<i>Forest and grassland</i>	0.004	-		
<i>Urban area</i>	0.001	-		
K	5-55	$kg\ h\ m^{-2}\ N^{-1}$	Varies spatially depending on soil texture	<i>Fiener et al., 2020</i>
P	0.85	-		<i>Fiener et al., 2020</i>
k_{iii}	350	$kg\ m^{-1}\ a^{-1}$		<i>Van Oost et al. 2006</i>

178

179 *2.3.2. MP contamination of soils*

180 Because sampling and sample analysis would be extremely time consuming and costly, it is not
 181 possible to determine the actual MP concentrations in a 390 km² catchment where estimates from MP
 182 inputs suggest large spatial heterogeneity. Hence, the potential soil-MP contamination needs to be
 183 estimated from the potential MP input from different sources. As soil erosion is dominant on arable land,
 184 an exclusive input estimate was performed for arable land. However, it is important to emphasize that
 185 most estimates are based on regional means for the whole of Bavaria and that any estimates of the MP
 186 accumulated in the catchment soils since the 1950s are based on a number of assumptions and
 187 simplifications, resulting in large uncertainties. To account for these uncertainties in the model outputs
 188 and arrive at a robust indication of the potential contribution of soil erosion as a source of MP in the
 189 stream network, we estimated the potential yearly mean, minimum and maximum soil-MP input for each
 190 input pathway (see below) and did separate and combined modelling runs for the different contamination
 191 estimates. As mentioned earlier, mean MP inputs from sewage sludge, compost and atmospheric
 192 deposition were estimated from means for all arable land in Bavaria, while input of tyre wear was derived



193 using catchment specific road data and road specific traffic data as far as possible. These represent the
194 typical sources in the agricultural landscape of Southern Germany, along with MP, applicable for
195 SPEROS-MP. Other potential MP input pathways, for instance from plastic used in agricultural
196 management (e.g. mulch films) or from littering, were not considered for two main reasons. (i) In Bavaria
197 mulch films are mostly associated with certain regions where specific crops or vegetables are grown,
198 especially asparagus. For our test site this is not the case, and using the average area of mulch cover in
199 Bavaria to estimate the potential mean input in the catchment would have resulted in very small input
200 amounts, not comparable with other regions in the world, where mulch films can be a very important
201 source of MP (Li et al., 2022; Liu et al., 2014). (ii) Larger macroplastic fragments from mulch films and
202 littering should only be transported with severe rill and ephemeral gully erosion, which are not the
203 dominant erosion processes in the region.

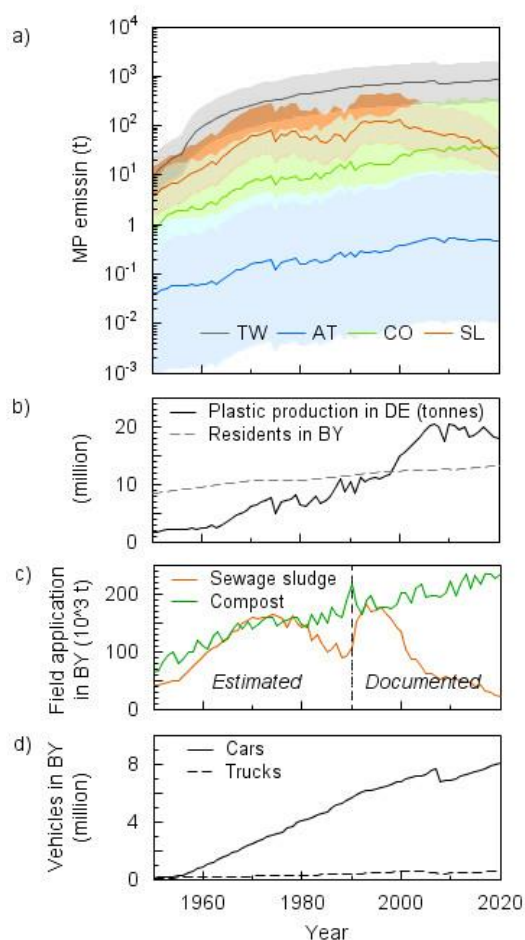
204 *2.3.3. Sewage sludge and compost*

205 Sewage sludge and compost as soil amendments (organic fertilizers) contain different quantities of
206 microplastic and, in the case of compost, small macroplastic. The first step was to estimate the amount
207 of sewage sludge and compost applied on Bavarian agricultural soils since 1950. Bavarian waste reports
208 (LfU, 1990-2020) allowed us to determine the mean annual input on arable land for the time period
209 1990–2020. Historical application rates of compost were determined based on a linear relationship
210 between application rates and population numbers between 1990 and 2020 (the variability was continued
211 at random) (LfStAD, 2022) (Fig. 2b, c). In the case of sewage sludge, the number of residents connected
212 to the sewage system was taken into account (Schleypen, 2017). The gaps between historical individual
213 values were interpolated. The development of plant technology and the use of sewage sludge between
214 1945 and 1990 were considered, as described by Schleypen (2017). While compost was constantly used
215 as an organic fertilizer, the use of sewage sludge was quite variable over time (Fig. 2c). From 1970



216 onwards new wastewater treatment plant (WWTP) technology meant that the sewage sludge was no
217 longer allowed to accumulate dry, but rather as wet sludge (Schleypen, 2017). This led to a sharp drop
218 in the use of sewage sludge as a fertilizer and it was not until the 1990s that it become popular again
219 (Fig. 2c). Since 2017, the application of sewage sludge has been largely banned in Bavaria (Schleypen,
220 2017).

221 The second step was to estimate the MP concentrations in sewage sludge and compost. To do this,
222 current literature values were used to estimate the MP concentrations for 2020. A minimum, mean and
223 maximum MP concentration was always considered, based on the range of values from literature. For
224 sewage sludge, data from Edo et al. (2020) were used; this is, to our knowledge, one of the few studies
225 providing a mass balance of MP for a WWTP by specifying the total wastewater volume and the total
226 amount of sewage sludge per day. The sum of the MP particles filtered out (contained in sewage sludge)
227 and the delivered MP from the WWTP effluent results in the number of MP detected in the WWTP input.
228 Edo et al. (2020) consider size classes 25–104 μm , 104–375 μm and 375–5,000 μm and their data show
229 that 95% of the MP in the WWTP is retained in the sewage sludge, which is consistent with other
230 publications giving ranges of 93–98% (Habib et al., 2020; Tang and Hadibarata, 2021; Unice et al.,
231 2019). For compost, data from Braun et al. (2021) were used, which contain all essential data on MP in
232 compost from Germany. They examined MP in the size ranges $< 1,000 \mu\text{m}$, 1,000–5,000 μm and $> 5,000$
233 μm . For the mass calculation of the MP in compost, macroplastics are also included.



234 **Figure 2: a) The MP emissions for arable land in Bavaria from the different sources, tyre wear**
235 **(TW), sewage sludge (SL), compost (CO) and atmospheric deposition (AT), from 1950 to 2020. b)**
236 **The development of plastics production in Germany and the population of Bavaria since 1950. c)**
237 **Amount of application of sewage sludge and compost as fertilizer on Bavarian arable land. d)**
238 **The number of registered cars and trucks in Bavaria since 1950.**
239

240



241 Both publications, Edo et al. (2020 and Braun et al. (2021, provide information on the size distribution
242 of the detected MP particles. This enabled the most accurate conversion possible between mass and
243 particle number. When converting, the particle size, size distribution and shape were taken into account.
244 While a spherical shape was assumed for sewage sludge, for compost the most realistic possible volume
245 for each detected particle was calculated (individual dimensions have been provided by the authors of
246 Braun et al. (2021). Based on the type of plastic detected, an average density of 1 was assumed for all
247 particles. An average MP load of 1.14 g MP kg⁻¹ dry matter of sewage sludge (min.: 0.42 g, max.: 4.04
248 g) and 0.15 g MP kg⁻¹ dry matter of compost (min.: 0.05 g, max.: 1.36 g) was assumed.

249 Based on the known amounts of sewage sludge and compost applied, it was possible to calculate the
250 corresponding amount of MP that ends up on Bavarian agricultural soils (kg m⁻²). When calculating the
251 MP concentration back to 1950, the amount of plastics produced in Germany was considered for each
252 year, as the MP concentration depends on the level of production (Fig. 2a, b). The annual amount of MP
253 was then evenly distributed across all agricultural fields in Bavaria, since spatial allocation within the
254 study area was not possible.

255 Between 1950 and 2020, a total of 7.26 million tonnes of sewage sludge and 11.7 million tonnes of
256 compost were added as organic fertilizer on agricultural fields in Bavaria. Hence it can be estimated that
257 4,090 t (min.: 1,510 t, max.: 14,500 t) and 1,110 t (min.: 358 t, max.: 10,100 t) of MP from sewage sludge
258 and compost, respectively, was dumped on arable land in Bavaria. From that, an average input on the
259 arable land in the Glonn River catchment of 42,100 kg MP from sewage sludge (min.: 15,500 kg, max.:
260 149,000 kg) and 11,500 kg MP from compost (min.: 3,660 kg, max.: 104,000 kg) was calculated. For
261 the arable land in the Glonn River catchment, this means an average annual MP application of 240 kg
262 MP from sewage sludge (min.: 90 kg, max.: 860 kg) and 370 kg from compost (min.: 120 kg, max.:



263 3,390 kg) in 2020 (Tab. 2). This results in a current entry rate of 1.14 mg MP m⁻² a⁻¹ (min.: 0.42 mg, 4.04
 264 mg) from sewage sludge and 1.75 mg MP m⁻² a⁻¹ (min.: 0.56 mg, max.: 15.8 mg) from compost.

265 **Table 2: MP inputs into arable soils within the test catchment, separated by different sources. All**
 266 **values are listed for the modelled time span 1950–2020 and separately for the year 2020.**
 267

	Tyre wear	Sewage sludge	Compost	Atmospheric deposition	Unit
1950–2020					
MP application to arable land	120,256	42,100	11,500	186	kg
min	43,969	15,500	3,660	4.30	
max	288,614	14,9000	104,000	4200	
2020					
MP application to arable land	3,109	240	370	4.76	kg
min	1,137	90	120	0.11	
max	7,462	860	3,390	107	
MP application rate	19.67	1.14	1.75	0.02	mg MP m⁻² a⁻¹
min	7.19	0.43	0.56	5*10 ⁻⁴	
max	47.2	4.08	16.03	0.45	

268

269 *2.3.4. Atmospheric deposition*

270 For the atmospheric deposition of MP, the data from four bulk deposition measurements (precipitation
 271 and dust deposition) in Bavaria (Witzig et al., 2021) were combined with the development of plastics
 272 production in Germany since the 1950s. As no better data were available it was assumed that the
 273 measured atmospheric deposition of MP in 2020 is proportional to German plastics production in general
 274 (Fig. 2a). This results in a mean cumulative atmospheric MP input on arable land in Bavaria of 18 tons
 275 of MP (min.: 0.41 t, max.: 407 t). Between 1950 and 2020, the arable land in the Glonn River catchment
 276 was loaded with a total of 186 kg of MP (min.: 4.20 kg, max.: 4,200 kg). For 2020 an average annual
 277 MP immission of 4.76 kg (min.: 0.11 kg, max.: 107 kg) or 0.02 mg MP m⁻² a⁻¹ (min.: 0.0005 mg, max.:
 278 0.5 mg) via atmospheric deposition was calculated (Tab. 2).



279 *2.3.5. Tyre wear*

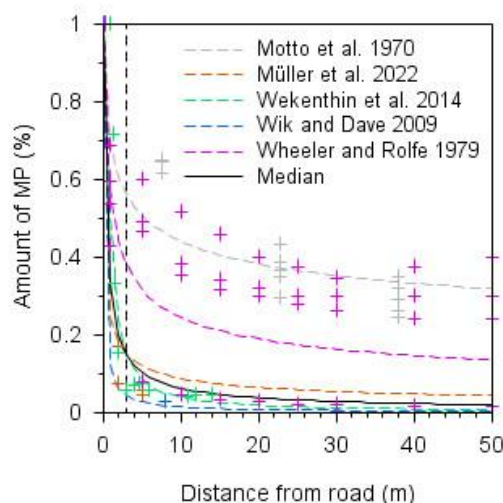
280 To determine the tyre wear particle input in the Glonn catchment we used existing traffic counting data
281 from 2005, 2010 and 2015 for the main roads (motorways, federal roads, state roads and district roads)
282 available from the Bavarian Road Information System (BAYSIS, 2015). Traffic volume for smaller roads
283 (except farm roads) in rural areas were derived from a 1 km x 1 km population density grid following
284 Gehrke et al. (2021). Based on these data the traffic volume (number of vehicles per km) for each paved
285 road in the Glonn catchment could be estimated for the years 2005, 2010 and 2015. This was done
286 separately for passenger cars (cars), heavy-duty vehicles (trucks) and motorcycles. For all other years,
287 the traffic volume (number of vehicles per km) per road was linearly extrapolated based on the traffic
288 volume in and the number of registered cars and trucks in Bavaria (LfStAD, 2022) (Fig. 2d). No emissions
289 from unpaved roads and agricultural machinery were considered.

290 A minimum, medium and maximum scenario was considered, based on the quantity of released tyre
291 particles specified in the literature. A mean tyre wear emission factor of 90 mg TW km⁻¹ (min.: 53 mg,
292 max.: 200 mg) was assumed for cars (a motorcycle represents half a car) and 700 mg TW km⁻¹ (min.:
293 105 mg, max.: 1,7*10³ mg) for trucks, based on the reviews of Hillenbrand et al. (2005 and Wagner et
294 al. (2018). Based on the length (km) and traffic volume (number of cars, motorbikes and trucks), the
295 released TW was calculated for each section of road.

296 The transport of TW from roads into the surrounding soil systems was estimated based on literature
297 information, assuming that the TW concentration exponentially declines with increasing distance from
298 the road (Fig. 3). However, we could only identify one study (Müller et al., 2022) that directly measured
299 TW contamination of soils with distance from the road, while most other studies (Motto et al., 1970;
300 Werkenthin et al., 2014; Wheeler and Rolfe, 1979; Wik and Dave, 2009) used chemical markers and the
301 distance from the road to estimate TW distribution. From all these different approaches we calculated a



302 median behaviour (Fig. 3). As the modelling is performed in a 5 m x 5 m grid, the land-use map may not
303 show all grass or vegetation strips often found along roads, which might lead to an overestimation of
304 TW input to arable land. Hence, we decided to use a conservative estimate, assuming that at least a 3 m
305 wide grass strip can be found on both sides of any road. Consequently about 85% of the TW produced
306 on any road (Fig. 3) cannot reach arable fields. The remaining 15% of TW that could potentially reach
307 arable land mostly settles within a 50 m distance from the road, whereas background MP concentrations
308 are reached in about 130 m distance (Fig. 3).



309
310

311 **Figure 3: The distribution of tyre wear in the soil relative to the distance from the road. Literature**
312 **values are based on direct detection of tyre wear (Müller *et al.* 2022) or on the estimated**
313 **concentrations of tyre wear particles based on chemical markers (Motto *et al.* 1970, Wheeler and**
314 **Dave 2009; Wik and Dave 2009; Wekenthin *et al.* 2014). The markers show the individual values,**
315 **the dashed lines show the mean of the respective reference. The black line represents the median**
316 **of all literature values used for modelling in this study.**

317

318 In comparison to the other MP sources considered (sewage sludge, compost and atmospheric deposition),
319 the estimate for TW was calculated on a field by field basis. To identify all agricultural fields affected



320 by road-borne TW deposits within a distance of 130 m, a land-use map was overlaid on the road network.
321 For each field, the area share of the associated road section and the distance to the road were considered
322 when calculating the TW load. The only limitation is that on fields affected by TW, in the model the
323 amount of TW was then distributed evenly over the entire field and not just on the affected field section
324 near the road (within 130 m).

325 Between 1950 and 2020, $120 \cdot 10^3$ kg tyre wear (min.: $44 \cdot 10^3$ kg, max.: $289 \cdot 10^3$ kg) ended up on
326 arable land in the Glonn catchment (Tab. 2). In 2020 the average annual MP application amounts to
327 $3.1 \cdot 10^3$ kg of tyre wear (min.: $1.1 \cdot 10^3$ kg, max.: $7.5 \cdot 10^3$ kg) (Tab. 2). The load from TW in 2020 can
328 reach maximum concentrations of $2.5 \cdot 10^3$ mg TW $\text{m}^2 \text{a}^{-1}$ on roads with heavy traffic use; the average
329 over all affected fields in the Glonn catchment area is 19.7 mg TW $\text{m}^2 \text{a}^{-1}$ (Tab. 2).

330 *2.4. Model validation*

331 It is obviously impossible to validate the modelled MP delivery to the stream network against measured
332 MP loads, as this would call for a continuous monitoring of MP delivery for several years at least.
333 However, the modelled sediment delivery can be validated against measured data from the Bavarian
334 State Office for Environment (Bayerisches Landesamt für Umwelt, LfU), which operated a discharge
335 and sediment monitoring gauge in Hohenkammer (Fig. 1) between 1968 and 2020. At this gauge with a
336 defined river cross-section, daily discharge was derived from continuous runoff depth measurements in
337 combination with a stage discharge rating curve, while the stationarity of this rating curve at the
338 measuring cross-section was randomly checked once or twice every year. At the gauging station a weekly
339 water sample was collected (1968–2020) and its sediment concentration was determined in the
340 laboratory. From 2011 onwards a turbidity probe (Solitax ts-line; Hach Lange GmbH; Germany) was
341 installed and regularly calibrated against the samples taken by hand. Based on the continuous discharge



342 and the weekly to continuous sediment concentration measurements, the LfU provided daily sediment
343 load data for the time span 1968 to 2020, which were aggregated to yearly values for this study.

344 *2.5. Modelled scenarios*

345 Apart from modelling and analysing the MP delivery to the stream network via the erosion pathway
346 for the period from 1950 to 2020, we also modelled three scenarios (S1 to S3) to discuss potential future
347 pathways up to 2100.

348 *Scenario S1 – business-as-usual scenario:* In this scenario it is assumed that the MP input to arable
349 land continues until 2100 with the same input rates estimated for 2020. Given the ongoing increase in
350 plastics production (Chia et al., 2021; Lwanga et al., 2022), this may even be a conservative estimate of
351 a business-as-usual scenario pathway.

352 *Scenario S2 – spatially targeted application of soil amendments:* This scenario addresses two aspects.
353 (i) A potential reduction of MP delivery to the stream network due to a targeted application of soil
354 amendments, keeping a distance of at least 100 m from the stream network in the case of compost and
355 sewage sludge application. (ii) More generally illustrating the sensitivity of MP delivery to the stream
356 network in the case of non-homogenous MP inputs in the catchment. For the latter, soil amendments
357 were solely applied in the vicinity of the stream network (max distance 100 m).

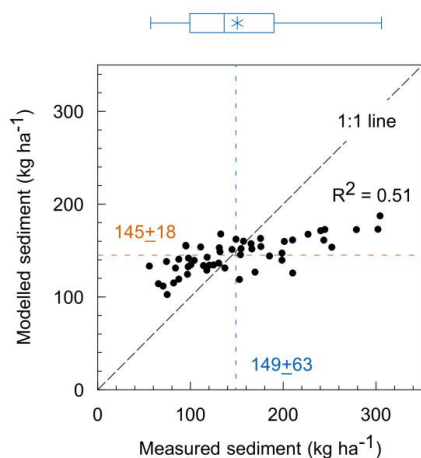
358 *Scenario S3 – stop MP input:* This scenario is set up to determine the extent to which soils function
359 as a long-term source for MP with regard to soil erosion, assuming the MP applied before 2020 remains
360 stable in the soil until 2100. Therefore, a potential decline in MP concentration in the plough layer either
361 results from a lateral loss to neighbouring land uses (grassland or forest) or the stream network, or is
362 buried below the plough layer due to deposition processes (here deposition due to water and tillage
363 erosion).



364 **3. Results**

365 *3.1. Sediment delivery*

366 Without any calibration, the model satisfactorily reproduced the measured long-term mean sediment
367 delivery of the Glonn outlet (Fig. 4). The modelled sediment deliveries resulted in a mean of 145 ± 18 kg
368 ha^{-1} , the measured mean contained 149 ± 63 kg ha^{-1} (Fig. 4). The model was obviously not able to
369 capture the full variability in the measured yearly sediment delivery ($R^2 = 0.51$; Fig. 4). It underestimates
370 years with high erosion rates, while it overestimates years with low erosion rates. However, we conclude
371 that the model performance (especially in reproducing the long-term mean) gives a solid basis for
372 modelling lateral MP fluxes due to erosion processes. Here it is important to note that our modelling
373 approach aims to estimate the magnitude of the MP erosion transport pathway, which was not analysed
374 in earlier studies, and that the estimated MP inputs contribute significantly to model uncertainty.



375 **Figure 4: Measured and modelled sediment delivery (1968 to 2020) at the outlet of the Glonn**
376 **catchment. The blue and orange lines represent the measured and modelled means, respectively.**
377 **The boxplots show the variability of the data. They show the median (line) and mean (star) and**
378 **the 1st and 3rd quartile, whiskers give the minimum and maximum.**
379



380 *3.2. MP erosion and delivery to stream network*

381 The constantly rising MP input to arable soils from different sources (Fig. 2) since 1950 is reflected
382 in the steadily increasing, erosion-induced MP delivery into the stream network (Fig. 5a). Due to the
383 long-term fertilization of arable land with sewage sludge, on average 0.51 kg of MP a⁻¹ entered the Glonn
384 stream network in 2020 (Tab. 3). For compost it is 0.77 kg of MP a⁻¹, with 0.01 kg of MP a⁻¹ from
385 atmospheric deposition (Tab. 3, Fig. 5a). With compost, sewage sludge and atmospheric deposition as
386 potential MP inputs to arable land, SPEROS-MP generated a total MP input into the stream network of
387 1.29 kg MP via the soil erosion pathway in 2020. Deliveries to the stream network have also steadily
388 increased in terms of TW (Fig. 5a), with an average 5.04 kg of MP a⁻¹ delivered to the stream network
389 in 2020 (Tab. 3).

390

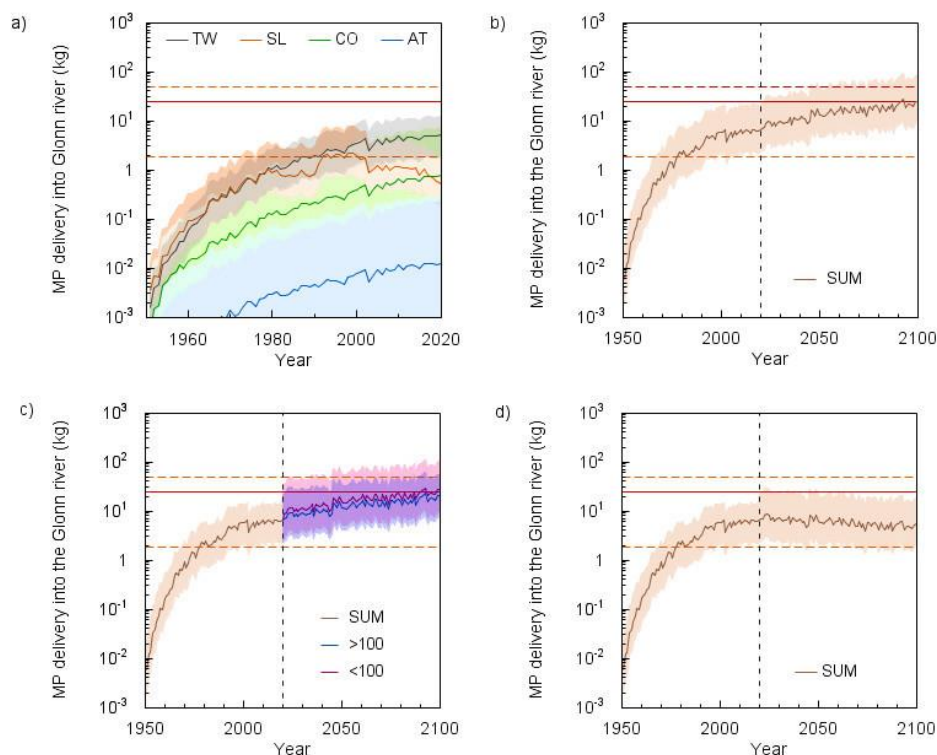


391 **Table 3: Soil erosion-induced MP delivery to the Glonn stream network, as well as redistribution**
 392 **to grassland and forest. The MP vertical loss below the plough layer is also given. All values are**
 393 **listed for the modelled time span 1950–2020 and separately for the year 2020.**
 394

	Tyre wear	Sewage sludge	Compost	Atmospheric deposition	Unit
1950–2020					
MP delivery into stream network	134	57	17	0.32	kg
min	49.0	21	5	0.01	
max	322	200	155	9	
<i>Percentage of MP application</i>	<i>0.11</i>	<i>0.14</i>	<i>0.15</i>	<i>0.17</i>	<i>%</i>
MP delivery into grassland	604	442	82	1.5	kg
min	221	163	24	0	
max	1,450	1,551	748	42	
<i>Percentage of MP application</i>	<i>0.50</i>	<i>1.05</i>	<i>0.71</i>	<i>0.81</i>	<i>%</i>
MP delivery into forest	108	97	18	0.34	kg
min	39.5	36	5	0	
max	259	340	164	10	
<i>Percentage of MP application</i>	<i>0.09</i>	<i>0.23</i>	<i>0.16</i>	<i>0.18</i>	<i>%</i>
MP loss below plough layer	4,703	2605	489	14.8	kg
min	1,720	961	144	6	
max	11,287	9,414	4,458	386	
<i>Percentage of MP application</i>	<i>3.91</i>	<i>6.19</i>	<i>4.25</i>	<i>8</i>	<i>%</i>
2020					
MP delivery into stream network	5.04	0.51	0.77	0.01	kg MP a⁻¹
min	1.84	0.2	0.2	0.0003	
max	12.1	1.8	7	0.3	

395

396



397

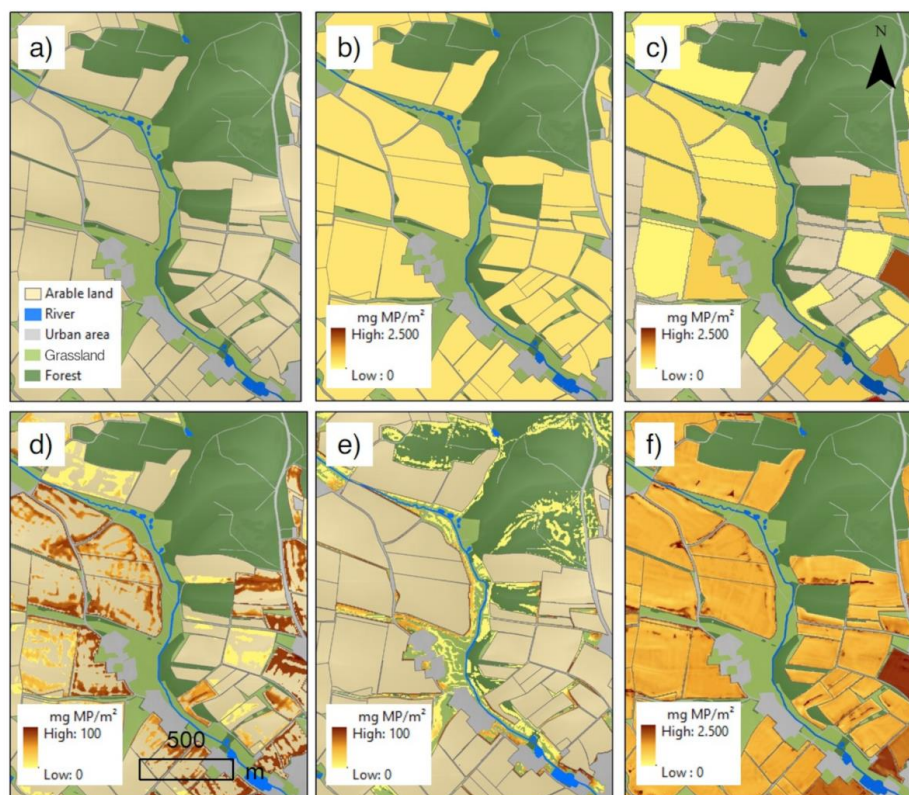
398 **Figure 5: MP delivery into the Glonn shown individually for tyre wear (TW), sewage sludge (SL),**
 399 **compost (CO) and atmospheric deposition (AT) or the sum of TW, SL, CO and AT (SUM). The**
 400 **dashed line gives the year 2020 as the starting point for different scenarios. For comparison, the**
 401 **amount of MP delivery through wastewater treatment plants (WWTP) in 2020 is shown as a red**
 402 **line (min. and max. as dotted lines). a) MP delivery into the Glonn river between 1950 and 2020.**
 403 **b) Result of scenario S1 with the assumption that the MP input will continue as in 2020. For**
 404 **comparison, the amount of MP delivery through wastewater treatment plants (WWTP) in 2020.**
 405 **c) Result of scenario S2. Compost and sewage sludge are applied to arable land at a distance of >**
 406 **100 m and < 100 m from water streams. d) Result of scenario S3 with no MP input at all from 2020**
 407 **onwards.**
 408



409 Between 1950 and 2020, 208.3 kg of MP (134 kg TW, 57 kg sewage sludge, 17 kg compost and 0.32
410 kg atmospheric deposition) entered the Glonn stream network (Tab. 3), while overall a sediment load of
411 $3.0 \cdot 10^8$ kg was delivered to the catchment outlet. TW was the main MP source, accounting for 64.3%,
412 followed by sewage sludge with 27.4%, compost with 8.2% and atmospheric deposition with 0.1%.
413 Taking into account the MP delivery relative to the MP input (i.e. total amount of MP input into soil in
414 1950–2020 vs. total MP delivery into the stream network from 1950–2020), only 0.14% of the MP
415 released to arable land was transported into the Glonn stream network. This differs slightly for the
416 different MP sources, ranging from 0.17% for atmospheric deposition to 0.11% for tyre wear (Tab. 3).

417 The spatially distributed model also allowed us to quantify the relocation of MP between different
418 land uses (an example is shown in Fig. 6f). The amount of MP delivered between 1950 and 2020 from
419 arable land to grassland and forest is $1.1 \cdot 10^3$ and $0.2 \cdot 10^3$ kg, respectively (Table 3). The larger delivery
420 to grasslands is particularly interesting, as these are mostly located along the stream network (see
421 discussion).

422 SPEROS-MP not only gives information about the MP relocation between arable land and other land
423 uses. The model also determines the amount of MP allocated below the plough layer (and thus out of
424 reach of water erosion) at depositional sites (an example is shown in Fig. 6e). Between 1950 and 2020,
425 3.9% of the TW supplied to arable land was moved below the plough layer (Tab. 3). This corresponds
426 to $4.7 \cdot 10^3$ kg MP or 35 times the amount reaching the stream network via water erosion. For sewage
427 sludge it is 6.19% ($2.6 \cdot 10^3$ kg), for compost 4.25% (489 kg) and for atmospheric deposition 8% (14.8
428 kg). Consequently, much more MP was translocated into the subsoil than was transported into the Glonn.
429 This transport into the subsoil was caused by water erosion (48.5%) and tillage erosion (51.5%).
430 Conversely, up to 95% of the MP applied to arable soil over the past 70 years remains in the plough layer
431 (infiltration and bioturbation excluded).



432

433 **Figure 6:** Example of catchment segment (for location see Figure 1) illustrating microplastic (MP)
434 input on arable land and results of erosion modelling between 1950 and 2020. The maps show the
435 situation in 2020. a) Field-based land use. b) Total MP input from sewage sludge, compost and
436 atmospheric input (without TW) as mean value over all arable land. c) MP input from TW,
437 spatially distributed to individual arable fields. d) MP concentration below plough layer. e) MP
438 transported to other land uses via soil erosion. f) MP distribution after water and tillage erosion
439 on arable land. (DEM © Bayerische Vermessungsverwaltung)

440



441 *3.3. Scenario S1 – business-as-usual*

442 If arable soils continue to be loaded with MP the same as in 2020, the annual MP delivery rate into the
443 Glonn stream network will increase by a factor of 4 by 2100. In 2100, 25.2 kg MP a⁻¹ (min.: 9.03 kg;
444 max.: 84.1 kg) through TW, compost, sewage sludge and atmospheric deposition would end up in the
445 stream network (Fig. 5b). Between 1950 and 2100, this would make a total MP input of 1.32 *10³ kg MP
446 (min.: 511 kg; max.: 4.7 *10³ kg) into the stream network.

447 *3.4. Scenario S2 – spatially targeted application of soil amendments*

448 In S2 MP inputs from atmospheric deposition and TW accumulation continued like in S1. However, the
449 location where the organic fertilizer (sewage sludge and compost) was applied in the catchment was
450 changed. All organic fertilizers were either applied at a distance of at least 100 m from the stream network
451 or within a distance smaller than 100 m along the stream network.

452 With an application at a distance of > 100 m, the MP delivery in the stream network would be reduced
453 to a total of 21.2 kg (min.: 7.72 kg; max.: 55.9 kg) in 2100 (Fig. 5c). That would correspond to a reduction
454 of 16% compared to S1. In the case of application at a distance of < 100 m, on the other hand, it would
455 be 27.9 kg (min.: 10 kg; max.: 102 kg) in 2100 and thus an increase of 10.7% compared to S1 (Fig. 5c).

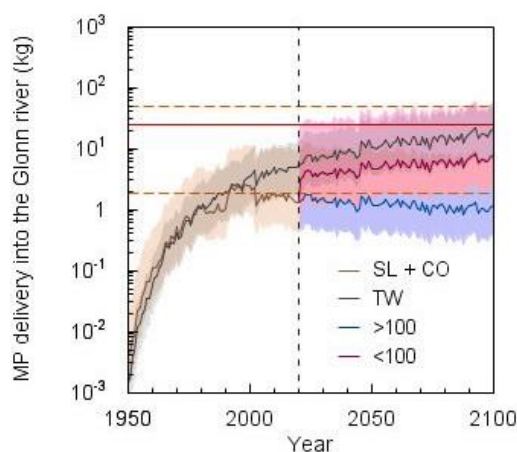
456 The result becomes clearer if we consider TW and the organic fertilizers separately. If the distance is >
457 100 m, the annual MP delivery rate from organic fertilizer (sewage sludge and compost) without TW is
458 1.1 kg MP a⁻¹ (min.: 0.4 kg, max.: 7.8 kg) in 2100 (Fig. 7). For 2100, this would result in a 78% reduction
459 of the annual MP delivery rate from organic fertilizer into water bodies compared to S1. In total from



460 1950 to 2100, 173 kg MP (min.: 60 kg; max.: $1.0 \cdot 10^3$ kg), or 46% less MP, from organic fertilizer would
461 end up in the stream network until 2100 (the effect of atmospheric input is negligible).

462 If organic fertilizer is applied along the stream network (max. distance < 100 m), a MP delivery of 7.8
463 kg a⁻¹ (min.: 2.6 kg, max.: 54 kg) is modelled in 2100 (Fig. 7). Between 1950 and 2100 a total of 493 kg
464 MP (min.: 168 kg; max.: $3.25 \cdot 10^3$ kg) would be delivered to the river system by organic fertilizer
465 (without TW).

466



467

468 **Figure 7: Result of scenario S2 individually shown for tyre wear (TW) and for sewage sludge**
469 **(SL) plus compost (CO) together as organic fertilizer applied to arable land at a distance of > 100**
470 **m and < 100 m from water streams. For comparison, the amount of MP delivery through**
471 **wastewater treatment plants (WWTP) in 2020 as red lines (min and max as dotted lines).**

472

473 3.5. Scenario S3 – stop MP input:

474 In scenario S3 MP input stops from 2020 onwards. This abrupt stop in plastic immission is not reflected
475 in the MP delivery rates after 2020 (Fig. 5d). However, in the year 2100, 5.43 kg of MP a⁻¹ (min.: 1.98
476 kg, max.: 18.2 kg) would still end up in the stream network from arable land due to soil erosion (Fig.



477 5d). This corresponds to a decrease in the annual MP delivery rate of 14% between 2020 and 2100, with
478 80 MP-free years (since 2020). Since 1950, a total of 684 kg MP (min.: 246 kg; max.: $2 \cdot 10^3$ kg) would
479 have ended up in the Glonn stream network.

480

481 **4. Discussion**

482 *4.1. Modelled erosion rates (sediment delivery)*

483 The modelling approach used, with a yearly time step and the missing temporal and spatial variability
484 of most model input data (especially the constant crop cover factor), while only varying yearly rainfall
485 erosivity, leads to model outputs that do not capture the full temporal dynamics of the measured yearly
486 sediment delivery (Fig. 4). It is well documented that averaging model input variables over space and
487 time generally leads to the overestimation of years with low sediment delivery and underestimation of
488 years with high sediment delivery (Keller et al., 2021; Meinen and Robinson, 2021). The reduced
489 temporal variability in modelled sediment delivery is expected for two main reasons: (1) the annual
490 model time step averages out years where individual extreme events dominate the yearly sediment
491 delivery, and (2) varying only the annual rainfall erosivity, while all other input parameters (especially
492 cropping dynamics) are kept constant, cannot capture the temporal dynamics. However, without any
493 model calibration the model almost perfectly reflects the long-term mean sediment delivery between
494 1968 and 2020 (Fig. 4), explaining 51% of the variability in the measured data. Hence, we conclude that
495 SPEROS-MP is robust enough for this modelling study which focusses on MP delivery to the stream
496 network in the Glonn catchment, especially as uncertainties associated with the erosion modelling are in
497 any case smaller than the uncertainties associated with estimates of MP immissions to the arable soils in
498 the catchment.



499 *4.2. Plausibility of MP soil input estimates*

500 Estimating the cumulative MP-soil immissions from different sources for a period starting from 1950
501 is of course associated with large uncertainties. To account for these uncertainties, we deliberately used
502 large ranges of possible inputs in our semi-virtual catchment approach which in the following discussion
503 are compared with literature values for Germany or Bavaria as a whole.

504 *4.2.1. MP from sewage sludge, compost and atmospheric deposition*

505 Brandes et al. (2021) calculated mean MP inputs into agricultural soils in Germany for compost (1990–
506 2016) and for sewage sludge (1983–2016). For Bavaria, their calculation results in compost-MP input
507 rates of between 15 and 80 mg MP m⁻² a⁻¹ and sewage sludge-MP input rates between 0 and 190 mg MP
508 m⁻² a⁻¹. Bertling et al. (2021) also determined MP immissions (TW excluded) to agricultural soils in
509 Germany, resulting in much higher input rates for 2021 for compost and sewage sludge, with up to 702
510 mg MP m⁻² a⁻¹ and 2.1*10³ mg MP m⁻² a⁻¹, respectively. In contrast to the first authors, Braun et al. (2021
511 calculate the possible MP load for the legally permissible amount of compost applied to fields in
512 Germany. This maximum permissible amount of compost application results in maximum possible entry
513 rates ranging from 34 to 4.7*10³ mg MP m⁻² a⁻¹ into agricultural soils via compost.

514 For this study, an MP emission to arable soils of between 0.42 and 4 mg MP m⁻² a⁻¹ for sewage sludge
515 and between 0.56 and 15.8 mg MP m⁻² a⁻¹ for compost were calculated for Bavaria. Our values are not
516 based on the maximum possible limits, but on the most realistic estimates possible. Therefore, our MP
517 loads remain well below the literature values. Nevertheless, the MP input from compost is likely to be
518 underestimated, based on optical detection of MP > 1 mm (Bläsing and Amelung, 2018; Braun et al.,
519 2021; Weithmann et al., 2018). Currently, much more compost (21*10⁷ t in 2020) is spread on fields in
520 Bavaria than sewage sludge (24*10⁴ t in 2020), causing higher MP emissions from compost (Fig. 2a).



521 This results from the reduction in sewage sludge application, which has been largely banned in Bavaria
522 since 2017 (Schleypen, 2017) (Fig. 2c). However, regional policy strategies regarding the use of sewage
523 sludge differ substantially within Germany, making comparisons within the country somewhat difficult
524 (Brandes et al., 2021).

525 For atmospheric deposition, an average of 771 and 395 MP particles $\text{m}^{-2} \text{d}^{-1}$ were measured at rural
526 locations in London and Hamburg (Klein and Fischer, 2019; Wright et al., 2019). Brahney et al. (2020
527 show that airborne microplastic particles accumulate at minimum concentrations of 48 ± 7 MP particles
528 $\text{m}^{-2} \text{d}^{-1}$ even in the most isolated areas of the United States (national parks and national wilderness areas).
529 Even in Antarctic snow up to 29 MP particles per melted litre were found (Aves et al., 2022). In this
530 study, the values of Witzig et al. (2021) were used to estimate the MP contribution via atmospheric
531 deposition. They made MP measurements at different locations in Bavaria, ranging from 74 ± 19 to
532 109 ± 16 MP particles $\text{m}^{-2} \text{d}^{-1}$. Even if the transfer of such particle numbers to mass inputs is associated
533 with additional uncertainties, these amounts are orders of magnitude smaller than the inputs from sewage
534 sludge and compost and hence less important.

535 *4.2.2. Tyre wear*

536 The large MP mass resulting from tyre wear is noticeable in both the TW input data and the TW
537 delivery rates into the stream network. With modelled mean TW delivery of 5 kg MP a^{-1} in 2020 into the
538 river system, the equivalent of half a car tyre ends up as MP in the Glonn (flow length of 50 km) each
539 year. However, the calculated mean TW input to the Glonn catchment of 200 mg MP m^{-2} in 2020 is in
540 same the range as the estimates in other studies. For example, annual values of between 180 and 370 mg
541 TW m^{-2} were reported for Germany (Baensch-Baltruschat et al., 2020; Kocher et al., 2010; Wagner et
542 al., 2018). The modelled MP input (see Fig. 3) to arable land in the Glonn catchment was substantially
543 smaller, with a mean of $19.7 \text{ mg TW m}^{-2}$.



544 Most of the TW remains on the roads or in the immediate vicinity. Some of the TW is expected to be
545 transported directly into surface waters via runoff from the road. Baensch-Baltruschat et al. (2020
546 estimated that 12–20% of the tyre wear released on German roads ends up in surface water via road
547 runoff. The hydrological model estimates of Unice et al. (2019 indicated that 18% of released tyre wear
548 was transported to freshwater in the Seine River catchment. In comparison, focusing on erosion of MP
549 which was mixed into the plough layer, only 0.11% of the applied TW to arable soils from 1950 to 2020
550 reached the river system. Although TW is the largest source of entry in our study, the MP flow to the
551 stream network is overall a conservative estimate. This mostly results from our assumption that all roads
552 are surrounded by a 3 m grass buffer strip (even if this was not shown in the 5 m x 5 m land-use raster
553 map used), always trapping at least 85% of the TW emissions (Fig. 3). Yet even this conservative
554 assumption is associated with high uncertainties. The width of the grass strip between the road and the
555 field has an enormous impact on the MP emission. A 2 m wide buffer strip would still retain
556 approximately 80% and a 1 m wide buffer strip approximately 65% of the TW emission (Fig. 3). Without
557 any assumed grass buffer strips, the MP emission from TW would be 8 times higher. Ultimately, the
558 spatially distributed tyre wear is still associated with uncertainties. The level of TW emissions into the
559 environment (not just arable land) makes other MP sources almost negligible, especially in terms of MP
560 saving strategies.

561 Overall, it can be concluded that our estimates of MP input to the Glonn catchment are in the same
562 order of magnitude, or somewhat smaller, compared to most other studies, and hence should be more or
563 less reasonable, even if any estimates are associated with large uncertainties (e.g. extrapolating back to
564 1950; the small number of studies available for estimating MP concentrations in sewage sludge and
565 compost; errors when transferring particle numbers in particle mass etc.). However, an error in modelling
566 the MP delivery into the stream network of the test catchment most likely results from the fact that mean
567 application rates (sewage sludge, compost) for the whole of Bavaria were used (Fig. 6b), while only TW



568 input was calculated on a catchment-specific basis (Fig. 6c). Again, it is important to note that the Glonn
569 catchment was used as an exemplar to address and discuss the potential magnitude of the MP/soil erosion
570 pathway in such mesoscale catchments determined by arable land use.

571 *4.3. The modelled fate of MP*

572 As a mass-balanced model, SPEROS-MP calculates the MP input in mass (kg m²) and not in particle
573 numbers. Hence, the model does not consider the type, shape, density, size or chemical properties of the
574 MP particles from different MP sources. It thus treats the erodibility of MP from all input pathways
575 equally. However, it can be assumed that particle properties play a decisive role for the erosion-induced
576 lateral transport, as well as for the potential vertical transport. Small MP particles should be translocated
577 faster below the plough layer due to bioturbation and maybe infiltration (Li et al., 2021; Rehm et al.,
578 2021; Waldschläger and Schüttrumpf, 2020). A subsequent reduction in MP concentration in the plough
579 layer will also reduce MP erosion. On the other hand, smaller MP particles might more strongly interact
580 with soil organic or mineral particles, or might even be included in soil aggregates, hence are more likely
581 transported as bulk soil. For example, Rehm et al. (2021) were able to demonstrate in a long-term plot
582 experiment that smaller PE particles (53–100 µm) are less strongly enriched in delivered sediments
583 compared to larger PE particles (250–300 µm). Such behaviour might change again with increasing
584 particle size, because if particles transported with sheet flow are larger than the flow depths (mostly < 1
585 mm), transport in suspension is no longer possible.

586 In general, the potential decrease in topsoil MP concentration due to infiltration and bioturbation is
587 not accounted for in SPEROS-MP. Vertical MP transport via infiltration and bioturbation has been
588 widely discussed and partially observed in earlier studies, e.g. (Rillig et al., 2017), while earthworms
589 play an especially important role in directly transporting MP via digestion and excretion (Huerta Lwanga



590 et al., 2017) or in preparing preferential flow pathways for MP leaching (Yu *et al.*, 2019). Ignoring these
591 processes of vertical movement below the plough layer will potentially lead to a slight overestimation of
592 the topsoil MP concentration in the modelling approach presented here.

593 SPEROS-MP not only delivers MP into the stream network, but also redistributes MP within the
594 catchment and within the soil profile. As arable land in the catchment is mostly found on the upper
595 slopes, and grassland in the flood plains, large amounts of MP are transported from arable land to
596 grassland (Tab. 3). No tillage takes place in grassland, leading to high MP concentration in the topsoil.
597 Along the main river in particular, grassland contaminated with MP (example shown in Fig. 6f) offers a
598 high potential for MP loss during flood events. In the flood plains, the groundwater level is regularly
599 close to the surface, hence the chance of MP leaching to the groundwater increases (Chia *et al.*, 2021;
600 Singh and Bhagwat, 2022; Viaroli *et al.*, 2022).

601 *4.4. Soil erosion as a potential MP source for inland waters*

602 Comparing the annual MP input to arable land and the annual MP loss through soil erosion indicates
603 that only a very small proportion ($\leq 0.17\%$ since 1950) is delivered to the stream network. The loss rate
604 of TW (0.11%) was the smallest compared to sewage sludge, compost and atmospheric deposition (Tab.
605 3). This is because the TW was not applied to all fields, but only to the fields next to a road. The low
606 percentage of input lost to the streams should not lead to the fallacy that MP transport via soil erosion is
607 negligibly small (Schell *et al.*, 2022; Weber *et al.*, 2022). This becomes clearer when comparing the MP
608 input from soil erosion with the MP input from wastewater treatment plants (WWTP) in the study area
609 (Fig. 5). Based on the known number and size of the WWTPs in the study area and MP loads in German
610 WWTPs from literature (Mintenig *et al.*, 2014), the MP delivery into the Glonn through WWTP outlets
611 can be estimated at an average of 25 kg MP a⁻¹ (min.: 1.9 kg, max.: 49 kg) in 2020 (Fig. 5). These values
612 represent a maximum scenario since the calculations were based on the possible full capacities of the



613 WWTPs. Within the test catchment, the MP delivery into the stream network was 6.3 kg MP a⁻¹ (min.:
614 2.2 kg, max.: 21 kg) in 2020, but (S1, Fig. 5b) could reach 25.2 kg MP a⁻¹ (min.: 9 kg, max.: 84.3 kg) by
615 the end of the century (Fig. 5b).

616 Rehm et al. (2021) have shown that due to its low density, MP is preferentially eroded and and is
617 enriched by up to a factor of four in delivered sediments. These potential enrichment effects were not included
618 in SPEROS-MP. In addition, other MP input sources such as plastic used in agriculture (e.g. mulch films)
619 and littering were not considered in this study. In this respect, therefore, the modelled MP delivery is a
620 conservative estimate. Overall, our results are in line with other, larger-scale model estimates for the
621 Bavarian section of the Danube catchment, showing that the MP input via soil erosion into water bodies
622 in rural areas outweighs the MP input of WWTP outlets (Witzig et al., 2021). It should therefore not be
623 claimed that soil erosion for MP transport is negligible (Schell et al., 2022) while wastewater treatment
624 plants are treated as a major MP source for inland waters (Cai et al., 2022; Eibes and Gabel, 2022;
625 Murphy et al., 2016).

626 *4.5. The MP sink function of soil results in a long-term MP source*

627 Today's MP pollution of arable land represents a long-term MP source for inland waters. With the
628 model scenarios S1 and S3, this study was able to show that the MP discharge from arable soils into
629 inland waters via soil erosion will still affect many generations to come, even if MP entry into the
630 terrestrial environment could be avoided. Because of low MP loss rates ($\leq 0.17\%$) via soil erosion and
631 the stability of conventional plastic materials over centuries (Ng et al., 2018), the MP particles
632 accumulate in the soil over the years. As most of the MP stays in the plough layer (Tab. 3), it is made
633 available to surface runoff and erosion processes on a regular basis. After 80 years without MP input in
634 S3, MP delivery from the soil decreased only by 14%. The MP concentration in the topsoil of arable land
635 decreases over time due to lateral MP loss into the stream network or into neighbouring grassland and



636 forest areas (example shown in Fig. 6f). The MP concentration in the topsoil also decreases since erosion
637 incorporates MP-free subsoil and, on the other hand, MP gets below the plough layer at depositional sites
638 (outside the range of water erosion). It is important to note that tillage erosion plays an important role,
639 as it supports the burial of MP below the plough layer (example shown in Fig. 6e).

640 S3 is reminiscent of other well-known environmental problems of long-term diffuse pollution, e.g.
641 with phosphorus (Daneshgar et al., 2018; Vaccari, 2009), where a pollutant accumulates in soils but
642 slowly find its way into inland waters through soil erosion. In this respect, it is important to note that it
643 will be easier to reduce MP inputs to stream networks coming from point sources, e.g. WWTP, whereas
644 the diffuse input will continue for centuries.

645 *4.6. Targeted application of MP-laden organic fertilizer*

646 The predicted increase in plastics production means that more MP inputs into the environment can be
647 expected in the future (Borrelle et al., 2020; Horton, 2022). Because of this, it is necessary to consider
648 what measures can be taken to reduce or avoid the entry of MP into the various environmental
649 compartments. The results of S2 have shown that the application of organic fertilizer (without TW)
650 containing MP at a distance of more than 100 m from the stream network can reduce MP entry into
651 surface waters via soil erosion by up to 46% compared to S1 (Fig. 7). By contrast (unplanned) application
652 of MP-laden soil amendments in the proximity of the stream network increase MP supply (by 53% in
653 our scenario).

654 This highlights the potential impact of optimized landscape management taking into account the
655 location of any agricultural management activity. It also shows that, in addition to soil conservation in
656 the field to prevent soil erosion, general changes in catchment management affecting hydrological and
657 sedimentological connectivity have important implications for the transport of sediments and pollutants.



658 Therefore, the location of soil additives, which are usually used to close production cycles, should be
659 considered for future use. This consideration can have a significant influence on the subsequent erosion
660 transport and redistribution of, for example, MP within a whole river catchment.

661 **5. Conclusion**

662 In this study, the transport of MP eroded from arable land was modelled across a mesoscale landscape.
663 Sewage sludge, compost, atmospheric deposition and tyre wear were considered as MP sources. Tyre
664 wear not only represented the largest MP input to arable land. It also generated the largest MP delivery
665 rates to the stream network — although tyre wear is not widespread on arable land, only occurring on
666 fields near the roads. In percentage terms, only a small fraction ($< 0.2\%$) of all MP applied to arable land
667 ended up directly in the stream network via soil erosion. However, the MP mass delivered into the stream
668 network represented a serious amount of MP input. The modelled MP delivery into the stream network
669 was in the same range of potential MP inputs from wastewater treatment plants from this rural area.

670 In addition, was shown that most of the MP applied to arable soils remains in the topsoil (0–20 cm)
671 for decades. Tillage produces a regular homogenization, and the MP stays available for surface runoff
672 and water erosion in the long term. Based on a series of scenarios modelled up to 2100 with no more MP
673 input from 2020 onwards, similar MP delivery rates (compared to 2020) could still be identified. This
674 implies that arable land represents an MP sink on the one hand and a long-term MP source for inland
675 waters on the other.

676 Using the soil profile update component included in the SPEROS-MP model, the MP concentrations
677 along the soil profile could be determined to a depth of 1 m. It was modelled that 5% of the MP applied
678 to arable land is translocated into the subsoil (> 20 cm) by tillage and water erosion. Located below the
679 plough horizon, the MP is out of reach for future lateral surface runoff erosion processes. Based on the



680 spatially distributed erosion model, it was also demonstrated that most of the eroded MP leaving arable
681 land is deposited in grassland (1% of applied MP). Especially in areas of the river valleys, these
682 accumulations could represent a concentrated MP entry into the stream network in the event of a flood.

683 The most effective protection for arable land would probably be to limit or ban the application of MP-
684 contaminated organic fertilizers. The following measures would be conceivable to protect water bodies
685 from MP inputs through soil erosion. Our model scenario showed that the targeted application of MP-
686 contaminated organic fertilizer at a distance of at least 100 m from the water body led to a significantly
687 lower MP delivery rate from this MP source. The deliberate creation of grass strips in the landscape to
688 protect against erosion would also be an option. However, it is important to consider that all calculated
689 and modelled cases were dominated by tyre wear, which is difficult to manage, especially in regions with
690 a high population and dense road network. Therefore, in order to preserve soil as a valuable resource, as
691 well as to protect the terrestrial and aquatic ecosystem from MP pollution and its effects, we should focus
692 on limiting MP emissions to the environment in general as much as possible.

693



694 **Competing interests**

695 Some authors are members of the editorial board of journal SOIL. The peer-review process
696 was guided by an independent editor, and the authors have also no other competing interests
697 to declare.

698 **Acknowledgments**

699 The authors would like to acknowledge the financial support from the Federal Ministry of Education
700 and Research towards this research as part of the initiative Plastics in the Environment (funding number
701 02WPL1447A-G). In addition, we would like to thank the Bavarian State Office of Agriculture (LfL)
702 and the Bavarian State Office for the Environment (LfU) for providing and accessing Bavaria-wide data,
703 as well as providing the modelling data for the Glonn catchment area. Finally, special thanks go to the
704 members of the Soil and Water Resources Research Group in Augsburg for supporting this work.

705



706 **References**

707

- 708 Accinelli C, Abbas HK, Bruno V, Vicari A, Little NS, Ebelhar MW, et al. Minimizing abrasion losses from film-
709 coated corn seeds. *Journal of Crop Improvement* 2021; 35: 666-678.
- 710 Auerswald K, Fiener P, Dikau R. Rates of sheet and rill erosion in Germany—A meta-analysis. *Geomorphology*
711 2009; 111: 182-193.
- 712 Aves AR, Revell LE, Gaw S, Ruffell H, Schuddeboom A, Wotherspoon NE, et al. First evidence of microplastics
713 in Antarctic snow. *The Cryosphere* 2022; 16: 2127-2145.
- 714 Baensch-Baltruschat B, Kocher B, Kochleus C, Stock F, Reifferscheid G. Tyre and road wear particles-A
715 calculation of generation, transport and release to water and soil with special regard to German roads.
716 *Science of The Total Environment* 2020; 752: 141939.
- 717 BAYSIS BS. *Straßenverkehrszählungen (SVZ)*. 2015.
- 718 Bertling J, Zimmermann T, Rödiger L. Kunststoffe in der Umwelt: Emissionen in landwirtschaftlich genutzte Böden.
719 *Fraunhofer UMSICHT* 2021: 220.
- 720 Bläsing M, Amelung W. Plastics in soil: Analytical methods and possible sources. *Science of the Total*
721 *Environment* 2018; 612: 422-435.
- 722 Borrelle SB, Ringma J, Law KL, Monnahan CC, Lebreton L, McGivern A, et al. Predicted growth in plastic waste
723 exceeds efforts to mitigate plastic pollution. *Science* 2020; 369: 1515-1518.
- 724 Borthakur A, Leonard J, Koutnik VS, Ravi S, Mohanty SK. Inhalation risks of wind-blown dust from biosolid-
725 applied agricultural lands: Are they enriched with microplastics and PFAS? *Current Opinion in*
726 *Environmental Science & Health* 2022; 25: 100309.
- 727 Brahney J, Hallerud M, Heim E, Hahnenberger M, Sukumaran S. Plastic rain in protected areas of the United States.
728 *Science* 2020; 368: 1257-1260.
- 729 Brandes E. Die Rolle der Landwirtschaft bei der (Mikro-) Plastik-Belastung in Böden und Oberflächengewässern.
730 2020.
- 731 Brandes E, Henseler M, Kreins P. Identifying hot-spots for microplastic contamination in agricultural soils—a
732 spatial modelling approach for Germany. *Environmental Research Letters* 2021; 16: 104041.
- 733 Brandhuber R, Auerswald K, Lang R, Müller A, Treisch M. ABAG interaktiv, Version 2.0. Bayerische
734 Landesanstalt für Landwirtschaft, Freising. 2018.
- 735 Braun M, Mail M, Heyse R, Amelung W. Plastic in compost: Prevalence and potential input into agricultural and
736 horticultural soils. *Science of The Total Environment* 2021; 760: 143335.
- 737 Bullard JE, Ockelford A, O'Brien P, Neuman CM. Preferential transport of microplastics by wind. *Atmospheric*
738 *Environment* 2021; 245: 118038.
- 739 Cai Y, Wu J, Lu J, Wang J, Zhang C. Fate of microplastics in a coastal wastewater treatment plant: Microfibers
740 could partially break through the integrated membrane system. *Frontiers of Environmental Science &*
741 *Engineering* 2022; 16: 1-10.
- 742 Chia RW, Lee J-Y, Kim H, Jang J. Microplastic pollution in soil and groundwater: a review. *Environmental*
743 *Chemistry Letters* 2021; 19: 4211-4224.
- 744 Colin G, Cooney J, Carlsson D, Wiles D. Deterioration of plastic films under soil burial conditions. *Journal of*
745 *Applied Polymer Science* 1981; 26: 509-519.
- 746 Corcoran PL. Degradation of microplastics in the environment. *Handbook of Microplastics in the Environment*.
747 Springer, 2022, pp. 531-542.
- 748 Daneshgar S, Callegari A, Capodaglio AG, Vaccari D. The potential phosphorus crisis: resource conservation and
749 possible escape technologies: a review. *Resources* 2018; 7: 37.
- 750 Desmet P, Govers G. A GIS procedure for automatically calculating the USLE LS factor on topographically
751 complex landscape units. *Journal of soil and water conservation* 1996; 51: 427-433.
- 752 Długoś V, Fiener P, Van Oost K, Schneider K. Model based analysis of lateral and vertical soil carbon fluxes
753 induced by soil redistribution processes in a small agricultural catchment. *Earth Surface Processes and*
754 *Landforms* 2012; 37: 193-208.
- 755 DWD DW. Klimadaten direkt zum Download. 3. Rasterfelder für Deutschland. 2020.



- 756 Edo C, González-Pleiter M, Leganés F, Fernández-Piñas F, Rosal R. Fate of microplastics in wastewater treatment
757 plants and their environmental dispersion with effluent and sludge. *Environmental Pollution* 2020; 259:
758 113837.
- 759 Eibes PM, Gabel F. Floating microplastic debris in a rural river in Germany: Distribution, types and potential
760 sources and sinks. *Science of The Total Environment* 2022; 816: 151641.
- 761 Feuilloley P, César G, Benguigui L, Grohens Y, Pillin I, Bewa H, et al. Degradation of polyethylene designed for
762 agricultural purposes. *Journal of Polymers and the Environment* 2005; 13: 349-355.
- 763 Fiener P, Dluogoß V, Van Oost K. Erosion-induced carbon redistribution, burial and mineralisation - Is the episodic
764 nature of erosion processes important? *Catena* 2015; 133: 282-292.
- 765 Fiener P, Dostál T, Krása J, Schmaltz E, Strauss P, Wilken F. Operational USLE-Based Modelling of Soil Erosion
766 in Czech Republic, Austria, and Bavaria—Differences in Model Adaptation, Parametrization, and Data
767 Availability. *Applied Sciences* 2020; 10: 3647.
- 768 Fiener P, Govers G, Van Oost K. Evaluation of a dynamic multi-class sediment transport model in a catchment
769 under soil-conservation agriculture. *Earth Surface Processes and Landforms* 2008; 33: 1639-1660.
- 770 Fiener P, Wilken F, Aldana-Jague E, Deumlich D, Gómez J, Guzmán G, et al. Uncertainties in assessing tillage
771 erosion—how appropriate are our measuring techniques? *Geomorphology* 2018; 304: 214-225.
- 772 Gehrke I, Dresen B, Blömer J, Sommer H, Lindow F, Röckle R. TyreWearMapping. Digitales Planungs-und
773 Entscheidungsinstrument zur Verteilung, Ausbreitung und Quantifizierung von Reifenabrieb in
774 Deutschland. Schlussbericht. 2021.
- 775 Govers G, Vandaele K, Desmet P, Poesen J, Bunte K. The role of tillage in soil redistribution on hillslopes.
776 *European Journal of Soil Science* 1994; 45: 469-478.
- 777 Guo J-J, Huang X-P, Xiang L, Wang Y-Z, Li Y-W, Li H, et al. Source, migration and toxicology of microplastics
778 in soil. *Environment International* 2020; 137: 105263.
- 779 Habib RZ, Thiemann T, Al Kendi R. Microplastics and wastewater treatment plants—a review. *Journal of Water
780 Resource and Protection* 2020; 12: 1.
- 781 Heinze WM, Mitrano DM, Cornelis G. Bioturbation-driven transport of microplastic fibres in soil. *Copernicus
782 Meetings*, 2022.
- 783 Hillenbrand T, Toussaint D, Boehm E, Fuchs S, Scherer U, Rudolphi A, et al. Discharges of copper, zinc and lead
784 to water and soil. Analysis of the emission pathways and possible emission reduction measures; Eintraege
785 von Kuper, Zink und Blei in Gewaesser und Boeden. Analyse der Emissionspfade und moeglicher
786 Emissionsminderungsmaßnahmen. 2005.
- 787 Horton AA. Plastic pollution: When do we know enough? *Journal of Hazardous Materials* 2022; 422: 126885.
- 788 Huerta Lwanga E, Thapa B, Yang X, Gertsen H, Salanki T, Geissen V, et al. Decay of low-density polyethylene
789 by bacteria extracted from earthworm's guts: A potential for soil restoration. *Sci Total Environ* 2017; 624:
790 753-757.
- 791 Hurley RR, Nizzetto L. Fate and occurrence of micro(nano)plastics in soils: Knowledge gaps and possible risks.
792 *Current Opinion in Environmental Science & Health* 2018; 1: 6-11.
- 793 Keller B, Centeri C, Szabó JA, Szalai Z, Jakab G. Comparison of the applicability of different soil erosion models
794 to predict soil erodibility factor and event soil losses on loess slopes in Hungary. *Water* 2021; 13: 3517.
- 795 Klein M, Fischer EK. Microplastic abundance in atmospheric deposition within the Metropolitan area of Hamburg,
796 Germany. *Science of the Total Environment* 2019; 685: 96-103.
- 797 Knight LJ, Parker-Jurd FN, Al-Sid-Cheikh M, Thompson RC. Tyre wear particles: an abundant yet widely
798 unreported microplastic? *Environmental Science and Pollution Research* 2020: 1-10.
- 799 Kocher B, Brose S, Feix J, Görg C, Peters A, Schenker K. Stoffeinträge in den Straßenseitenraum-Reifenabrieb.
800 BERICHT DER BUNDESANSTALT FUER STRASSENWESEN. UNTERREIHE
801 VERKEHRSTECHNIK 2010.
- 802 Krasa J, Dostal T, Van Rompaey A, Vaska J, Vrana K. Reservoirs' siltation measurements and sediment transport
803 assessment in the Czech Republic, the Vrchlice catchment study. *Catena* 2005; 64: 348-362.
- 804 LfStad BfSuD. Statistisches Jahrbuch für Bayern. 2022.
- 805 LfU BLfU. Abfallwirtschaft—Hausmüll in Bayern—Bilanzen 2002. Bayerisches Landesamt für Umweltschutz,
806 Augsburg 1990-2020.



- 807 Li H, Lu X, Wang S, Zheng B, Xu Y. Vertical migration of microplastics along soil profile under different crop
808 root systems. *Environmental Pollution* 2021; 278: 116833.
- 809 Li S, Ding F, Flury M, Wang Z, Xu L, Li S, et al. Macro-and microplastic accumulation in soil after 32 years of
810 plastic film mulching. *Environmental Pollution* 2022; 300: 118945.
- 811 Lian J, Liu W, Meng L, Wu J, Zeb A, Cheng L, et al. Effects of microplastics derived from polymer-coated fertilizer
812 on maize growth, rhizosphere, and soil properties. *Journal of Cleaner Production* 2021; 318: 128571.
- 813 Liu EK, He WQ, Yan CR. ‘White revolution’ to ‘white pollution’—agricultural plastic film mulch in China.
814 *Environmental Research Letters* 2014; 9.
- 815 Lwanga EH, Beriot N, Corradini F, Silva V, Yang X, Baartman J, et al. Review of microplastic sources, transport
816 pathways and correlations with other soil stressors: a journey from agricultural sites into the environment.
817 *Chemical and Biological Technologies in Agriculture* 2022; 9: 1-20.
- 818 Meinen BU, Robinson DT. Agricultural erosion modelling: Evaluating USLE and WEPP field-scale erosion
819 estimates using UAV time-series data. *Environmental Modelling & Software* 2021; 137: 104962.
- 820 Mintenig S, Int-Veen I, Löder M, Gerdtz G. Mikroplastik in ausgewählten Kläranlagen des Oldenburgisch-
821 Ostfriesischen Wasserverbandes (OOWV) in Niedersachsen. 2014.
- 822 Motto HL, Daines RH, Chilko DM, Motto CK. Lead in soils and plants: its relation to traffic volume and proximity
823 to highways. *Environmental Science & Technology* 1970; 4: 231-237.
- 824 Müller A, Kocher B, Altmann K, Braun U. Determination of tire wear markers in soil samples and their distribution
825 in a roadside soil. *Chemosphere* 2022; 294: 133653.
- 826 Murphy F, Ewins C, Carbonnier F, Quinn B. Wastewater Treatment Works (WwTW) as a Source of Microplastics
827 in the Aquatic Environment. *Environ Sci Technol* 2016; 50: 5800-8.
- 828 Nadeu E, Gobin A, Fiener P, Van Wesemael B, Van Oost K. Modelling the impact of agricultural management on
829 soil carbon stocks at the regional scale: the role of lateral fluxes. *Global Change Biology* 2015: DOI:
830 10.1111/gcb.12889.
- 831 Nasser S, Azizi N. Occurrence and Fate of Microplastics in Freshwater Resources. *Microplastic Pollution*.
832 Springer, 2022, pp. 187-200.
- 833 Ng E-L, Lwanga EH, Eldridge SM, Johnston P, Hu H-W, Geissen V, et al. An overview of microplastic and
834 nanoplastic pollution in agroecosystems. *Science of the total environment* 2020; 627: 1377-1388.
- 835 Ng EL, Lwanga EH, Eldridge SM, Johnston P, Hu HW, Geissen V, et al. An overview of microplastic and
836 nanoplastic pollution in agroecosystems. *Science of the Total Environment* 2018; 627: 1377-1388.
- 837 Nunes JP, Wainwright J, Biëlders CL, Darboux F, Fiener P, Finger D, et al. Better models are more effectively
838 connected models. *Earth Surface Processes and Landforms* 2018; 43.
- 839 Pérez-Reverón R, González-Sálamo J, Hernández-Sánchez C, González-Pleiter M, Hernández-Borges J, Díaz-Peña
840 FJ. Recycled wastewater as a potential source of microplastics in irrigated soils from an arid-insular
841 territory (Fuerteventura, Spain). *Science of The Total Environment* 2022; 817: 152830.
- 842 Rehm R, Zeyer T, Schmidt A, Fiener P. Soil erosion as transport pathway of microplastic from agriculture soils to
843 aquatic ecosystems. *Science of The Total Environment* 2021; 795: 148774.
- 844 Rillig MC, Ziersch L, Hempel S. Microplastic transport in soil by earthworms. *Sci Rep* 2017; 7: 1362.
- 845 Sajjad M, Huang Q, Khan S, Khan MA, Yin L, Wang J, et al. Microplastics in the soil environment: A critical
846 review. *Environmental Technology & Innovation* 2022: 102408.
- 847 Schell T, Hurley R, Buenaventura NT, Mauri PV, Nizzetto L, Rico A, et al. Fate of microplastics in agricultural
848 soils amended with sewage sludge: Is surface water runoff a relevant environmental pathway?
849 *Environmental Pollution* 2022; 293: 118520.
- 850 Scheurer M, Bigalke M. Microplastics in Swiss Floodplain Soils. *Environmental science & technology* 2018.
- 851 Schleypen P. Abwasserbehandlung (nach 1945). *Historisches Lexikon Bayerns* 2017.
- 852 Schmidt J, v.Werner M, Michael A. Application of the EROSION 3D model to the CATSOP watershed, The
853 Netherlands. *Catena* 1999; 37: 449-456.
- 854 Schwertmann U, Vogl W, Kainz M. Bodenerosion durch Wasser. Ulmer Verlag, 64 p 1987.
- 855 Singh S, Bhagwat A. Microplastics: A potential threat to groundwater resources. *Groundwater for Sustainable
856 Development* 2022: 100852.
- 857 Sommer F, Dietze V, Baum A, Sauer J, Gilge S, Maschowski C, et al. Tire abrasion as a major source of
858 microplastics in the environment. *Aerosol and Air Quality Research* 2018; 18: 2014-2028.



- 859 Tang KHD, Hadibarata T. Microplastics removal through water treatment plants: Its feasibility, efficiency, future
860 prospects and enhancement by proper waste management. *Environmental Challenges* 2021; 5: 100264.
- 861 Tian L, Jinjin C, Ji R, Ma Y, Yu X. Microplastics in agricultural soils: sources, effects, and their fate. *Current*
862 *Opinion in Environmental Science & Health* 2022; 25: 100311.
- 863 Unice KM, Weeber MP, Abramson MM, Reid RCD, van Gils JAG, Markus AA, et al. Characterizing export of
864 land-based microplastics to the estuary - Part I: Application of integrated geospatial microplastic transport
865 models to assess tire and road wear particles in the Seine watershed. *Science of the Total Environment*
866 2019; 646: 1639-1649.
- 867 Vaccari DA. Phosphorus: a looming crisis. *Scientific American* 2009; 300: 54-59.
- 868 Van Oost K, Govers G, De Alba S, Quine T. Tillage erosion: a review of controlling factors and implications for
869 soil quality. *Progress in Physical Geography* 2006; 30: 443-466.
- 870 Van Oost K, Govers G, Desmet P. Evaluating the effects of changes in landscape structure on soil erosion by water
871 and tillage. *Landscape ecology* 2000; 15: 577-589.
- 872 Van Oost K, Govers G, Quine TA, Heckrath G, Olesen JE, De Gryze S, et al. Landscape-scale modeling of carbon
873 cycling under the impact of soil redistribution: The role of tillage erosion. *Global Biogeochemical Cycles*
874 2005a; 19.
- 875 Van Oost K, Quine T, Govers G, Heckrath G. Modeling soil erosion induced carbon fluxes between soil and
876 atmosphere on agricultural land using SPEROS-C. In: Roose EJ, Lal R, Feller C, Barthes B, Stewart BA,
877 editors. *Advances in soil science. Soil erosion and carbon dynamics*. CRC Press, Boca Raton, 2005b, pp.
878 37-51.
- 879 Van Rompaey AJ, Verstraeten G, Van Oost K, Govers G, Poesen J. Modelling mean annual sediment yield using
880 a distributed approach. *Earth Surface Processes and Landforms* 2001; 26: 1221-1236.
- 881 Verstraeten G, Prosser IP. Modelling the impact of land-use change and farm dam construction on hillslope
882 sediment delivery to rivers at the regional scale. *Geomorphology* 2008; 98: 199-212.
- 883 Viaroli S, Lancia M, Re V. Microplastics contamination of groundwater: Current evidence and future perspectives.
884 A review. *Science of The Total Environment* 2022: 153851.
- 885 Wagner S, Hüffer T, Klöckner P, Wehrhahn M, Hofmann T, Reemtsma T. Tire wear particles in the aquatic
886 environment-a review on generation, analysis, occurrence, fate and effects. *Water research* 2018; 139: 83-
887 100.
- 888 Waldschläger K, Schüttrumpf H. Infiltration Behavior of Microplastic Particles with Different Densities, Sizes,
889 and Shapes—From Glass Spheres to Natural Sediments. *Environmental Science & Technology* 2020; 54:
890 9366-9373.
- 891 Weber CJ, Santowski A, Chiffard P. Investigating the dispersal of macro-and microplastics on agricultural fields
892 30 years after sewage sludge application. *Scientific reports* 2022; 12: 1-13.
- 893 Weithmann N, Möller JN, Löder MG, Piehl S, Laforsch C, Freitag R. Organic fertilizer as a vehicle for the entry
894 of microplastic into the environment. *Science Advances* 2018; 4: eaap8060.
- 895 Werkenthin M, Kluge B, Wessolek G. Metals in European roadside soils and soil solution—A review.
896 *Environmental Pollution* 2014; 189: 98-110.
- 897 Wheeler G, Rolfe G. The relationship between daily traffic volume and the distribution of lead in roadside soil and
898 vegetation. *Environmental Pollution (1970)* 1979; 18: 265-274.
- 899 Wik A, Dave G. Occurrence and effects of tire wear particles in the environment—A critical review and an initial
900 risk assessment. *Environmental pollution* 2009; 157: 1-11.
- 901 Witzig C, Wörle K, Földi C, Rehm R, Reuwer A-K, Ellerbrake K, et al. Mikroplastik in Binnengewässern.
902 Untersuchung und Modellierung des Eintrags und Verbleibs im Donaugebiet als Grundlage für
903 Maßnahmenplanung. MICBIN Abschlussbericht. 2021.
- 904 WRB IWG. World reference base for soil resources 2014, update 2015. International soil classification system for
905 naming soils and creating legends for soil maps. World Soil Resources Reports No. 106. FAO 2015.
- 906 Wright S, Ulke J, Font A, Chan K, Kelly F. Atmospheric microplastic deposition in an urban environment and an
907 evaluation of transport. *Environment International* 2019: 105411.
- 908 Zhang L, Xie Y, Liu J, Zhong S, Qian Y, Gao P. An overlooked entry pathway of microplastics into agricultural
909 soils from application of sludge-based fertilizers. *Environmental science & technology* 2020; 54: 4248-
910 4255.



- 911 Zhang Y, Gao T, Kang S, Shi H, Mai L, Allen D, et al. Current status and future perspectives of microplastic
912 pollution in typical cryospheric regions. *Earth-Science Reviews* 2022; 226: 103924.
913 Zhao S, Zhang Z, Chen L, Cui Q, Cui Y, Song D, et al. Review on migration, transformation and ecological impacts
914 of microplastics in soil. *Applied Soil Ecology* 2022; 176: 104486.
915 Zhou Y, Wang J, Zou M, Jia Z, Zhou S. Microplastics in soils: A review of methods, occurrence, fate, transport,
916 ecological and environmental risks. *Science of The Total Environment* 2020: 141368.
917 Zubris KA, Richards BK. Synthetic fibers as an indicator of land application of sludge. *Environ Pollut* 2005; 138:
918 201-11.
919